AIP | APL Materials

Research Update: The electronic structure of hybrid perovskite layers and their energetic alignment in devices

Selina Olthof

Citation: APL Mater. **4**, 091502 (2016); doi: 10.1063/1.4960112
View online: http://dx.doi.org/10.1063/1.4960112
View Table of Contents: http://scitation.aip.org/content/aip/journal/aplmater/4/9?ver=pdfcov
Published by the AIP Publishing

Research Update: The electronic structure of hybrid perovskite layers and their energetic alignment in devices

Selina Olthof
Institute of Physical Chemistry, University of Cologne, Luxemburger Straße 116, 50939 Cologne, Germany

(Received 10 June 2016; accepted 19 July 2016; published online 1 August 2016)

In recent years, the interest in hybrid organic–inorganic perovskites has increased at a rapid pace due to their tremendous success in the field of thin film solar cells. This area closely ties together fundamental solid state research and device application, as it is necessary to understand the basic material properties to optimize the performances and open up new areas of application. In this regard, the energy levels and their respective alignment with adjacent charge transport layers play a crucial role. Currently, we are lacking a detailed understanding about the electronic structure and are struggling to understand what influences the alignment, how it varies, or how it can be intentionally modified. This research update aims at giving an overview over recent results regarding measurements of the electronic structure of hybrid perovskites using photoelectron spectroscopy to summarize the present status. [http://dx.doi.org/10.1063/1.4960112]

I. INTRODUCTION

Hybrid organic–inorganic perovskites are described by the crystal structure AMX_3, containing an organic cation A^+, a metal cation M^{2+}, and a halide X^-. In the past few years, this material has presented itself as a success story in the field of thin film photovoltaics where power conversion efficiencies could be improved at an unprecedented pace;[1] looking ahead, there is tremendous potential for other thin film applications like light emitting diodes or lasers.[2,3]

Three key factors can be identified that play crucial role for the further advancement of the field. First, the active material, i.e., the perovskite layer, has to be optimized regarding its bandgap and phase stability. The bandgap can be tuned from approximately 1.2 to 3.7 eV by interchanging or mixing in different halides (X = Cl, Br, I) or metals (M = Ge, Sn, Pb), while it was shown that the stability increases by (partially) replacing the organic cation methylammonium (MA) by formamidinium (FA) or Cs.[4] Second, the morphology plays an important role, as large crystals and homogeneous layer formation are essential for efficient charge transport and good diode characteristics; this can be widely influenced by (post-)processing conditions. The focus of this paper is on the third pillar, namely, the topic of optimizing the energy level alignment between the perovskite and the adjacent transport layers in order to facilitate efficient charge transport throughout a device. In order to be able to optimize barriers in a non-trial-and-error fashion, detailed knowledge about the positions of the perovskite conduction band (CB) minimum and valence band (VB) maximum are needed to be able to select matching transport layers. On top of this, at interfaces, shifts in the vacuum level position, i.e., interface dipoles, can occur due to, e.g., chemical reactions, charge transfer, and dipole orientation[5] or band bending might be present due to charge redistribution. Therefore, not only the individually measured energy values are relevant, but also the interface has to be investigated.

UV photoelectron spectroscopy (UPS) is the most widely applied technique to directly probe the occupied density of states (DOS) and work function (WF) of thin films by which the ionization energy (IE) can be extracted. By sequentially evaporating one material on top of the other, the alignment at the interface, e.g., dipole formation or the appearance of band bending, can be

accessed. The technique has therefore been increasingly applied over the last 2-3 years to look at hybrid perovskites. By combining UPS either with inverse photoelectron spectroscopy (IPES) or the measurement of the optical gap, the electron affinity (EA) can be calculated. The aim of this research update is to summarize the current status of hybrid perovskites with respect to UPS measurements. Other methods that can provide similar information, like X-ray photoelectron spectroscopy (XPS), photoelectron spectroscopy in air (PESA), or Kelvin probe, will not be included. The focus will be on measurements of the individual materials, the tuning of the perovskite work function, and the interface alignment to adjacent organic transport layers.

II. MEASUREMENTS OF THE DENSITY OF STATES OF PEROVSKITES

From the variety of possible hybrid perovskite materials, $MAPbI_3$ is the most studied system. The earliest UPS measurement was published in 2003 by Umebayashi *et al.*[6] where the authors studied the VB DOS and performed density functional theory (DFT) calculations to associate the observed features with the corresponding orbitals. They showed that only the metal and halide contribute to the states close to the band edges, while the orbitals originating from the organic cation lie deep within the bands. As shown in Fig. 1, the metal has an occupied s orbital (lone pair) whose electrons interact strongly with the in-plane anion p states forming an antibonding state as the top of the VB with mostly s-orbital character. The CB minimum is constituted from antibonding Pb(6p)-I(5p) states with a p orbital character.

With the rising interest in hybrid perovskite based solar cells in the past years, researchers started investigating the DOS of hybrid perovskites more extensively using UPS and by now more than 20 publications report such measurements on $MAPbI_3$.[7–30] Surprisingly, the reported values show a significant diversity, with reported values for the IE ranging from 5.1 to 6.65 eV. An overview that summarizes all published IE values of $MAPbI_3$ is shown in Fig. 2 in which a Gaussian fit to the data shows a mean value of IE = 5.6 eV; the detailed listing of the contributing papers and individual values can be found in Table S1 of the supplementary material.[31] This kind of spread is unknown in related fields of inorganic or organic semiconductors, where reported values typically agree within a few 100 meV.

It is important to rationalize the underlying reason for this strong variation, as it would be important for the research community to reach a consensus. It has been shown by several research groups that the stoichiometric composition, influenced by preparation conditions, changes the measured ionization energy.[15,25,27] In our own work in Ref. 27, we investigated more than 40

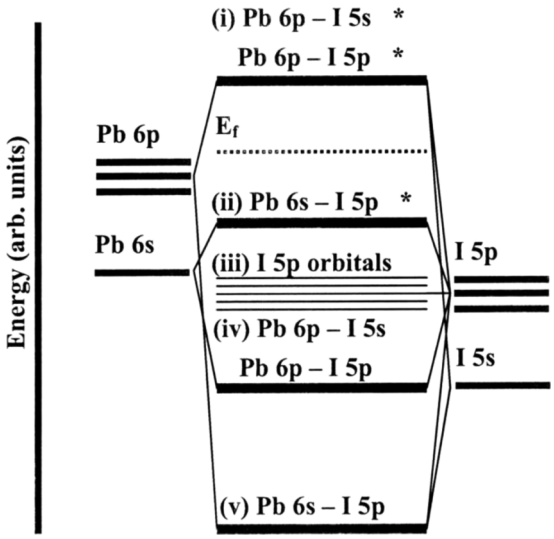

FIG. 1. Bonding diagram of a $[PbI_6]^{-4}$ cluster, representing the perovskite $MAPbI_3$. Reproduced with permission from Umebayashi *et al.*, Phys. Rev. B **67**, 2 (2003). Copyright 2003 American Physical Society.

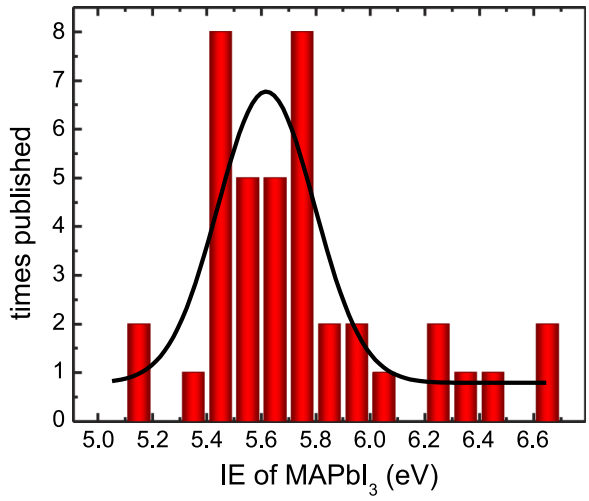

FIG. 2. Statistical distribution of IE values reported in the literature with the values taken from Refs. 7–30. For a more detailed listing see Table S1 of the supplementary material.[31] The black curve marks a Gaussian fit to the data.

$MAPbI_3$ films and observed that the IE can be tuned between 5.7 and 6.4 eV when varying the processing conditions and/or the precursor mixing ratios. Figure 3 shows the dependence of the IE on the lead to nitrogen ratio, which is representative for interstitials incorporated in the film. The linear relation with respect to the film stoichiometry shows that excess of MA^+ in the perovskite film leads to lower IE, while an excess of Pb^+/PbI_2 leads to higher values. Films with a correct stoichiometry, e.g., prepared from a co-solution of PbI_2 and MAI at molar ratio 1:1, were found to have an intermediate IE of 6.05 eV. Similar experiments by Kim *et al.* showed a variation in IE values between 5.5 eV and 6.2 eV.[15]

Another cause for the wide variety of reported values lies in differences regarding the data evaluation. Commonly in the related field of organic semiconductors, the onset of the transport level is determined by taking the linear slope to the DOS at the band edge and extracting the value at the intersection with the background intensity. In perovskites, different approaches have been established, ranging from taking the linear slope to using the onset in a semi-logarithmically scaled plot, or looking for the first faint appearance of DOS in the bandgap. These three methods will yield vastly different values for the valence band onset (E_{VB}), varying by about 1 eV, as discussed in greater detail in the supplementary material.[31] The motivation for using the faint onset and

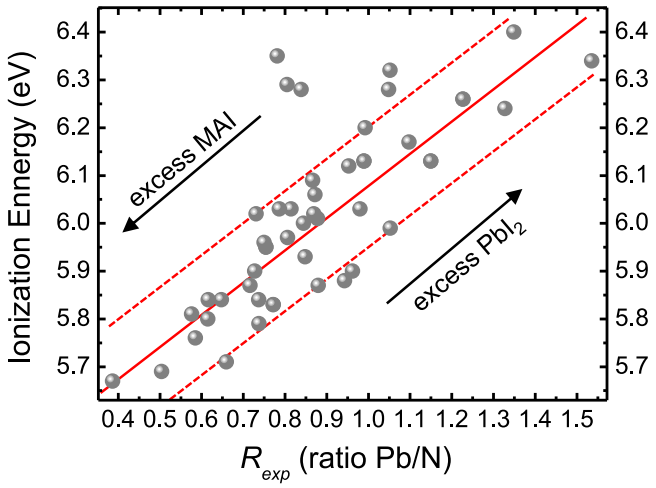

FIG. 3. Dependence of the IE of $MAPbI_3$ perovskite films on the layer composition, which can be deduced from the elemental ratio of Pb (from PbI_2) and N (from MAI). Adapted from Emara *et al.*, Adv. Mater. **28**, 553 (2016). Copyright 2016 Wiley.

semi-logarithmic scale values is based on the fact that otherwise values for the hole injection barrier are sometimes larger than the bandgap of the material, therefore underestimating the relevant states close to the onset, as was recently discussed in a paper by Endres *et al.*[32] However, the measurement of both the log scale onset and the faint onset of the DOS depend significantly on the experimental setup, i.e., signal to noise ratio or dynamic range of the detector (see Fig. S2 of the supplementary material for examples).[31] Therefore the linear onset is the only reproducible value that can then be compared between different research groups; such a consistency can be considered to be more important than adjusting the readout method to produce more expected values.

Lately, increasing focus is laid on hybrid perovskite systems other than $MAPbI_3$ or mixed perovskites in order to optimize the bandgap or increase the film stability. The effects these substitutions have on modifying the optical band gap are well studied. The same is, unfortunately, not true for the induced changes in valence or conduction band position, i.e., IE and EA. Theoretical calculations suggest that the antibonding VB orbital is very sensitive to the metal-halide bond length while the CB is rather insensitive. Therefore the VB (and thereby the band gap) can be tuned by changing the size of the cation A in the perovskite crystal. It has to be noted, however, that only in a cubic crystal a smaller bond length, i.e., a smaller cation, leads to larger orbital overlap and therefore to a smaller bandgap; in tetragonal or orthorhombic crystals, the smaller cation leads to a stronger tilting of the crystal structure, thereby actually decreasing the orbital overlap.[33] For the M site substitution, on the other hand, mainly the CB position should be affected due to changes in the ionic/covalent nature of the M–X bond.[34] However, anomalous trends have been reported due to changes in spin-orbit coupling when switching from Pb → Sn → Ge or resulting changes in crystal structure.[35–37] Regarding the X-site substitution in the lead based perovskite system, Butler *et al.* predicted that the bandgap increase from I to Cl is mainly due to a VB downward shift, while CB upshift is less pronounced.[38] On the other hand, Buin *et al.* calculate for the same material system and halide substitution equal changes in VB and CB.[39]

With respect to optimizing device architectures, especially for choosing adequate transport materials, it is important to know if the observed changes in band gap are due to a shift in the VB, or in CB, or an equivalent change of both. The publications on UPS measurements of hybrid perovskites other than $MAPbI_3$ are limited and, of course, prone to the same systematic inconsistencies as described for the case of $MAPbI_3$. Therefore, the following discussion will be mostly limited to work that report comparative studies between different perovskite systems, so that the relative changes should be consistent, independent of the data evaluation procedure.

Currently, there are no UPS studies available comparing the A site substitution, e.g., MA^+ vs. FA^+. Koh *et al.*[40] measured an IE of 5.7 eV for $FAPbI_3$ which is well within the distributions of values published for $MAPbI_3$. Regarding halide substitution, both, Schulz *et al.*[28] and Li *et al.*,[16] found that by switching the halide from $MAPbI_3$ to $MAPbBr_3$ or preparing mixed Br/I perovskites, the shift in bandgap is mostly due to a change in IE and therefore the position of the VB, while the CB does not move significantly. This implies that the same electron transport layer can be used in both cases; however, the HTL has to be modified to compensate for the change in bandgap. In addition, Li *et al.* studied Cl and mixed I/Cl systems. When comparing $MAPbI_3$ with $MAPbCl_3$, they found an upward shift of the CB by 300 meV and a downward shift of the VB by ~1 eV, so in contrast to the mixed I/Br systems, here both energy levels seem to change. Another study in which the halide was exchanged was performed using the tin based $MASnI_3$ and $MASnBr_3$.[41] Here, ionization energies of 5.47 and 5.54 eV were found for the two materials, therefore almost identical values. In this case, and contrary to the Pb based perovskites, the band gap increase (ΔE_g = 0.85 eV) seems to be due to a change in the CB.

Regarding the metal substitution, a comparative study of $MAPbI_3$, $MASnI_3$ as well as mixed Pb/Sn systems was published by Hao *et al.*[30] Here, they found no difference in the IE of the pure Sn and Pb based perovskite (5.47 and 5.45 eV, respectively), indicating that the observed change in bandgap of 200 meV must take place in the CB. However, for the intermediate mixing ratios, they observed a downward movement of the VB and an increase in IE to 5.77 eV. At the same time, the optical band gap decreased, so both CB and VB change due to the mixing. This corresponds to the anomalous band gap behavior mentioned above induced by variations in spin-orbit coupling as well as changes in crystal structure.[36]

III. INFLUENCE OF THE SUBSTRATE ON THE PEROVSKITE ALIGNMENT AND WORK FUNCTION

To estimate the alignment within the solar cell and rationalize device performances, mostly vacuum level alignment between the substrate and the perovskite layer is assumed, so individually determined IE and EA values are matched at the interfaces. This would correspond to the Schottky-Mott limit, meaning that the perovskite work function (Wf_P) is identical to the substrate work function (Wf_S) and can therefore be tuned while the Fermi energies (E_F) do not align. This is, however, not necessarily true. Interface dipoles can form due to a variety of effects like permanent dipole moments that align at the interface or chemical interactions that are taking place. Second, band bending can occur inside the perovskite layer, in case there is a sufficient charge carrier density present in the semiconductor to align the substrate and perovskite Fermi levels.

To study this effect, Millers *et al.*[21] investigated $MAPbI_3$ on top of various materials like PEDOT:PSS, NiO, Cu_2O, Al_2O_3, ZnO, ZrO_2, and FTO using UPS and XPS. They found a shifting of the valence band position relative to the Fermi energy as a function of substrate type; on n-type substrates, the CB was pinned at the Fermi level ($Wf_P \sim 3.8$ eV) while on p-type substrates, the Wf increased and the Fermi energy was in a mid-gap position ($Wf_P \sim 4.9$ eV). This implies that the substrate is, to some degree, able to control the band alignment of $MAPbI_3$, at least for the relatively thin layer thicknesses investigated here. In a different study, Schulz *et al.*[22] compared thick layers of $MAPbI_3$ on the high Wf material NiO ($Wf_S = 4.9$ eV) and the low Wf TiO_2 ($Wf_S = 4$ eV). They found a change in perovskite Wf of 700 meV, corresponding to a shift from a mid-gap Fermi energy position on the p-type NiO to a position close to the CB for n-type TiO_2. Finally, Correa Baena *et al.* compared higher Wf SnO_2 ($Wf_S = 4.46$ eV) and lower Wf TiO_2 ($Wf_S = 4.02$ eV) and found a difference of 130 meV in the respective positions of the Fermi energy in the perovskite bandgap.[11] However, the perovskite showed an opposing trend with a lower Wf value of $Wf_P = 4.0$ eV on the SnO_2 compared to the one on TiO_2 ($Wf_P = 4.13$ eV). This strongly suggests that not only the Wf but also the nature of the substrate might influence the interface alignment, most likely through the formation of an interface dipole.

To further elucidate the interplay between substrate and perovskite, it is worthwhile to again compare individual values reported in the literature. Figure 4 summarizes the available data taken from Refs. 7, 8, 10–13, 16–26, and 28 which are used to relate Wf_S and Wf_P; again, the detailed listing of values can be found in Table S1 of the supplementary material.[27] There is only a slight correlation between the two values, indicated by the shaded area; however, scattering of the data points is clearly dominant; for the same substrate material (e.g., PEDOT:PSS at $Wf_S = 5.1$ eV)

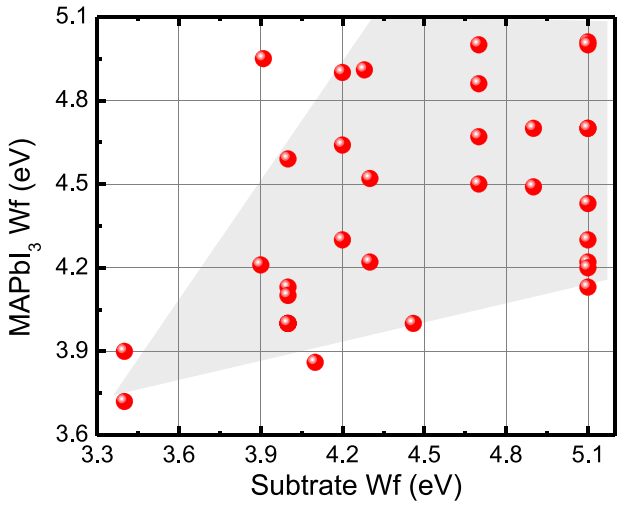

FIG. 4. Literature survey of published values of $MAPbI_3$ work functions depending on the work function of the substrate using Refs. 7, 8, 10–13, 16–26, and 28. Detailed information on the values can be found in Table S1 of the supplementary material.[31]

different values are reported. This could be due to several factors: (i) air exposure of the film between preparation and measurement could lead to a shift of E_F due to unintentional oxygen doping (see, e.g., supplementary material of Ref. 27) or modification of the crystal structure/DOS by water incorporation. (ii) An influence of film stoichiometry and therefore preparation on the measured work function have been reported by Wang *et al.*[24] They showed that by tuning the precursor mixing ratio, the work function of $MAPbI_3$ on PEDOT:PSS could be changed from 4.8 eV (MAI rich) to 4 eV (PbI_2 rich) which was supported by theoretical calculations[42] predicting that Pb vacancies in an MAI rich film act as p-dopants which shift the Fermi energy downward while I vacancies in a PbI_2 rich film induce n-doping, thereby moving E_F upward. (iii) Finally, if band bending occurs within the perovskite, then the value extracted for a thin film will differ from a thicker film. The intrinsic charge carrier density is reported to be rather low, in the range of $10^9 - 5 \times 10^{11}$ cm^{-3} for $MAPbI_3$[30,43,44] and 10^{14} cm^{-3} for $MASnI_3$.[30] A simple estimate using the Poisson equation to describe the formation of a depletion region and using average values of carrier density (10^{-10} cm^{-3}), built in field (V_B = 1.5 eV), and permittivity (ε = 60) yields values for a depletion region in the range of 1 μm. This is by a factor of 2-3 larger than the typical device thickness but nonetheless it can be expected that band bending plays a role.

To study interface dipoles and bend bending that might be present in the perovskite, interface resolved measurements have to be performed. The research on these interfaces is challenging as it is necessary to stepwise and reproducibly prepare thin (~nm thick) perovskite layers and measure the evolution of the vacuum level and valence band onset with increasing thickness; this is only possible using vapor phase deposition. Recently, the first study in this regard has been published looking at the interface between the low Wf substrate ZnO (Wf_S = 3.6 eV) and $MAPbI_3$.[26] Here, Zhou *et al.* stepwise evaporated the perovskite on top of a single crystal surface, ranging in thickness from 1.5 to 190 nm. They indeed found a strong upward interface dipole of 1.2 eV due to a thin PbI_2 interface layer created by a partial decomposition of the perovskite. This is followed by quick downward shift of the vacuum level by 0.5 eV, once the perovskite starts to form; the final Wf_P is 4.3 eV. There was almost no change observed in VB onset with layer thickness; therefore, no significant band bending took place, possibly due to the fact that the CB band is right away close to the Fermi energy and no built in field is created.

IV. ENERGETIC ALIGNMENT TO ORGANIC TRANSPORT LAYERS

Two common device architectures are employed for perovskite solar cells. On one hand,TiO_2 is used as electron extraction layer in combination with a 2,2′-7,7′-tetrakis(*N*,*N*-di-*p*-methoxyphenylamine)-9,9′-spirobifluorene (spiro-MeOTAD) hole extraction layer while the inverted design usually contains a PEDOT:PSS anode and a phenyl-C61-butyric acid methyl ester (PCBM) electron extraction layer. In such devices, two types of unfavorable barriers can be present: extraction barriers can appear at interfaces between the absorbing layer and the transport layer when its transport level is further away from the Fermi energy than the transport level of the perovskite. Extraction barriers lead to a loss in current around the open circuit voltage V_{oc} (S-kink in IV-curve) and a lower fill factor. Injection barriers, on the other hand, do not lead to reduced current; however, they reduce the V_{oc} of a device by limiting the Fermi level splitting (see, e.g., Ref. 45 for more detailed discussion). Therefore, it is very important to ensure matching of the transport levels throughout a device.

The interface to the top contact organic transport material is easier to study by UPS, as some of these materials are by default evaporated in vacuum, so a stepwise build-up of the interface is possible. Some of the published studies that will be discussed in the following are based on actual device architectures while others can be considered to be more general studies, looking at various organics to establish trends in the alignment. Non-organic top contact interfaces, like the alignment to Au[19] or MoO_3,[18,46] have been investigated but will not be further considered here. Throughout this discussion, it has to be kept in mind that the perovskite preparation conditions are likely to influence the measured interface alignment, and differences in data evaluation can lead to different conclusions regarding the relative positions of the energy levels.

The first study on such an alignment was reported by Schulz *et al.* for spiro-MeOTAD evaporated on top of $MAPbI_3$ and $MAPbBr_3$.[28] The authors found a small injection barrier of 400 meV

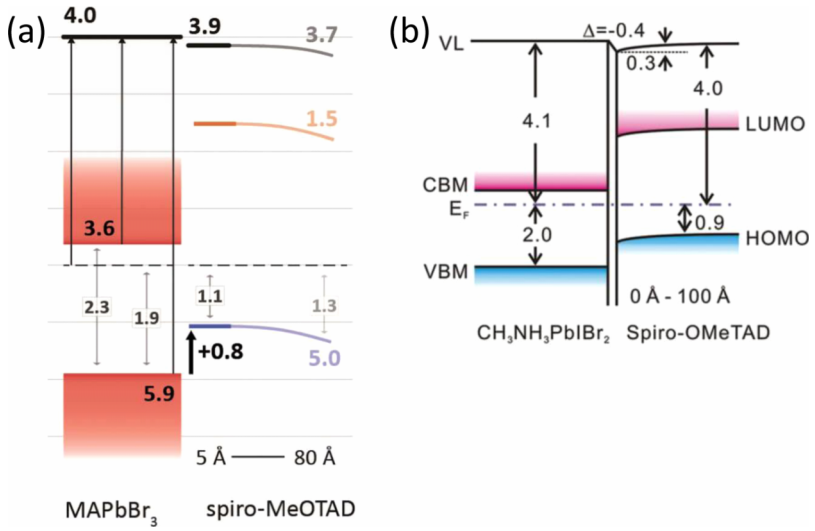

FIG. 5. Experimentally measured energy level diagrams for the interface to spiro-MeOTAD for (a) $MAPbBr_3$ and (b) $MAPbIBr_2$. In both cases, the organic layer was evaporated on top of a solution processed perovskite layer. (a) is reprinted with permission from Schulz *et al.*, Energy Environ. Sci. **7**, 1377 (2014). Copyright 2014 Royal Society of Chemistry. (b) is reprinted with permission from Wang *et al.*, Adv. Mater. Interfaces **2**, 1400528 (2015). Copyright 2015 Wiley.

from the VB of $MAPbI_3$ into the highest occupied molecular orbital (HOMO) of spiro-MeOTAD, which should result to an equivalent loss in V_{oc}. For the corresponding interface with $MAPbBr_3$, shown in Fig. 5(a), a larger injection barrier of 0.8 eV was found, due to the deeper VB of the bromide compound, clearly making spiro-MeOTAD a poor choice for these wide band gap active layers. A very similar energy level offset of 0.8 eV was found by Wang *et al.*,[46] who studied the interface between the mixed perovskite $MAPbIBr_2$ and spiro-MeOTAD as shown in Fig. 5(b). Between these two publications, there are, however, differences regarding the appearance of an interface dipole in case of the mixed halides and the direction of observed band bending in the organic layer which is once downward (a) and once upward (b), possibly due to differences in unintentional doping of the spiro-MeOTAD film.

Several studies focusing on the inverted solar cell structure followed, looking at the contact to organic electron extraction layers. Due to the possibility for evaporation, the fullerene C_{60} was mostly chosen instead of PCBM which is more commonly used in solar cell devices. Using UPS and IPES measurements, Schulz *et al.*[22] found flat band conditions and a good alignment between the lowest unoccupied molecular orbital (LUMO) of C_{60} and the CB of $MAPbI_3$ with a mere injection barrier of 100 meV, as shown in Fig. 6(a). In combination with a hole blocking barrier of ~1 eV, this looks like an ideal interface for selective electron extraction out of the active material.

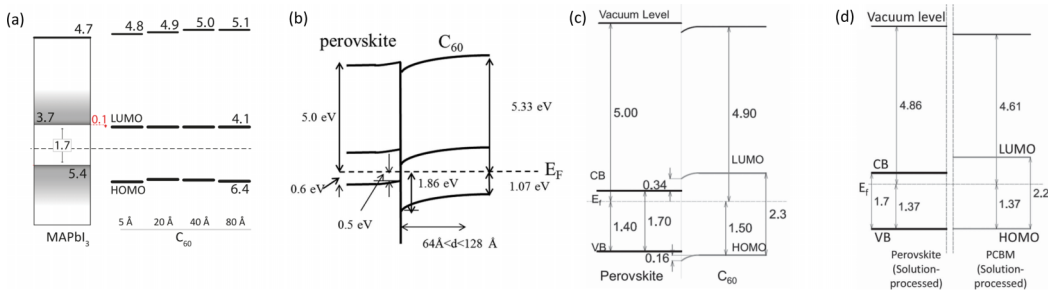

FIG. 6. Experimentally determined interface alignments between $MAPbI_3$ and the fullerene C_{60} (a)–(c) and between $MAPbI_3$ and fullerene PCBM (d). (a) is reprinted with permission from Schulz *et al.*, Adv. Mater. Interfaces **2**, 1400532 (2015). Copyright 2015 Wiley. (b) is reprinted with permission from Wang *et al.*, Appl. Phys. Lett. **106**, 111603 (2015). Copyright 2015 AIP Publishing LLC. (c) and (d) are reprinted with permission from Lo *et al.*, Adv. Funct. Mater. **25**, 1213 (2015). Copyright 2015 Wiley.

Wang *et al.*,[47] on the other hand, observed for the same material combination a rather different alignment as shown in Fig. 6(b). At the interface, the LUMO of C_{60} is positioned well within the bandgap of the perovskite, introducing an injection barrier of ~1 eV which should significantly reduce the achievable V_{oc}. With increasing C_{60} coverage, an upward bending of the transport levels by 800 meV occurs accompanied by an upward shift of the perovskite DOS, indicating an electron transfer into the C_{60} layer. Third, Lo *et al.*[20] observed in their UPS measurements a staggered interface as shown in Fig. 6(c), so the LUMO of C_{60} at the interface is positioned 340 meV above the perovskite CB, leading to an extraction barrier of 340 meV while the HOMO is below the VB of the perovskite, so no hole blocking should be achieved. In addition, there is a small band bending of 160 meV in the C_{60}, further hindering charge extraction. Nonetheless, a device built with this interface worked reasonably well (PCE 6.4%). In the same publication, the authors looked at the interface to PCBM, by spin coating two fairly thin layers on top of $MAPbI_3$ (0.5 and 10 nm); the resulting energy level diagram is shown in Fig. 6(d). The interface alignment is very similar to C_{60}, so again an electron extraction barrier is found and no hole blocking behavior.

These discrepancies in the measurement data and the resulting variations in the interpretation of the working mechanism of this device relevant interface are again to a large degree due to differences in UPS data evaluation, i.e., regarding the readout of the VB onset position. While all studies find the same IE for C_{60} (IE = 6.4 eV), the values for the $MAPbI_3$ vary from 5.4 to 6.4 eV.

Last year, an extensive study was published by Wang and co-workers[45] based on the mixed perovskite $MAPbIBr_2$, where the interface to a wider range of molecules was investigated to study their relative energy level positions. Depending on the organic band gap and the IE/EA values, a variety of different alignments were achieved. These included, e.g., the staggered hetero-interfaces (with spiro-OMeTAD as shown in Fig. 5(b) as well as NPB) which at the same time offer efficient hole extraction and good electron blocking behavior. Furthermore, they found that in case the EA of the organic film is larger than the Wf of the perovskite, a strong interface dipole and band bending occurs that shifts the LUMO above the Fermi level by a charge transfer from the organics to the perovskite. This way a straddling gap was created with the low band gap $F_{16}CuPc$ and a reverse staggered-gap with the large band gap HAT-CN. The creation of such pinning at interfaces could be a promising way to ensure barrier-free charge extraction.

Thibau *et al.* looked as well at a variety of small molecules on $MAPbI_3$, including m-MTDATA, NPB, CBP, Alq_3, and TPBi.[29] Here, no interface resolved measurements were performed, but very thin organic layers (1 nm) were deposited to probe the interface band positions. As they had troubles reproducibly measuring the vacuum level position of the perovskite (most likely due to changes in IE with sample preparation), they restricted themselves to look at the distance of the organics HOMO to the perovskites VB onset. From the linear relation between this offset and the IE of the respective organic film, they conclude that vacuum level alignment is predominant, so no significant interface dipoles occurred. Similarly, Chen *et al.* found vacuum level alignment for CuPc deposited on $MAPbI_3$.[10]

V. SUMMARY

Currently, there are strong discrepancies in the reported UPS data due to variations in processing as well as differences in data evaluation. No clear picture has emerged yet about the absolute values of the ionization energy and electron affinity of the different perovskite materials, and therefore, rather little can be concluded about the relative energy level shifts responsible for the variability in bandgap when changing the crystal composition.

Regarding the alignment between the substrate and the deposited perovskite, it can be concluded that different values for the perovskite work function have been reported; thus, the injection barriers and the position of the Fermi energy inside the semiconductor bandgap can be changed to some degree by the substrate. However, scattering of data points dominates and no clear correlation can be established, yet. The reasons could either be variations in interface dipole formation, unintentional self-doping, or the appearance of band bending. The fact that for $MAPbI_3$ often a pinning of the Fermi energy on the conduction band is reported indicates that this material could be predominantly n-type.

Finally, interesting work has been done regarding the investigation of interfaces to various organic transport materials. Even though rather dissimilar alignments are found, even for the same material combinations, it seems that in many cases, vacuum level alignment is fulfilled. This means that the offsets between energy levels at this interface could be estimated from individually measured ionization energy and electron affinity values.

For the future, there is a strong need for more rigorous and consistent data evaluation, which, in the opinion of the author, has to be based on taking linear extrapolation to the density of states in the UPS data. Clearly, more comparative studies are needed to establish general trends for different perovskite materials and it will be of great interest to more extensively investigate the novel mixed perovskites to understand their higher efficiency in devices, which could be due to morphology, stability, or maybe an increase in DOS or better alignment to the transport layers. So, we can be sure that hybrid perovskite will continue to be an exciting playing field for solid state researchers in the coming years.

[1] National Renewable Research Laboratory, NREL Efficiency Chart, http://www.nrel.gov/, 2015.
[2] H. Cho, S.-H. Jeong, M.-H. Park, Y.-H. Kim, C. Wolf, C.-L. Lee, J. H. Heo, A. Sadhanala, N. Myoung, S. Yoo, S. H. Im, R. H. Friend, and T.-W. Lee, Science **350**, 1222 (2015).
[3] M. Saba, M. Cadelano, D. Marongiu, F. Chen, V. Sarritzu, N. Sestu, C. Figus, M. Aresti, R. Piras, A. Geddo Lehmann, C. Cannas, A. Musinu, F. Quochi, A. Mura, and G. Bongiovanni, Nat. Commun. **5**, 5049 (2014).
[4] D. P. McMeekin, G. Sadoughi, W. Rehman, G. E. Eperon, M. Saliba, M. T. Hörantner, A. Haghighirad, N. Sakai, L. Korte, B. Rech, M. B. Johnston, L. M. Herz, and H. J. Snaith, Science **351**, 151 (2016).
[5] N. Koch, ChemPhysChem **8**, 1438 (2007).
[6] T. Umebayashi, K. Asai, T. Kondo, and A. Nakao, Phys. Rev. B **67**, 2 (2003).
[7] A. Calloni, A. Abate, G. Bussetti, G. Berti, R. Yivlialin, F. Ciccacci, and L. Duò, J. Phys. Chem. C **119**, 21329 (2015).
[8] J. Chang, H. Zhu, B. Li, F. H. Isikgor, Y. Hao, Q. Xu, and J. Ouyang, J. Mater. Chem. A **4**, 887 (2016).
[9] J. Chang, H. Zhu, J. Xiao, F. H. Isikgor, Z. Lin, Y. Hao, K. Zeng, Q.-H. Xu, and J. Ouyang, J. Mater. Chem. A **4**, 7943 (2016).
[10] S. Chen, T. W. Goh, D. Sabba, J. Chua, N. Mathews, C. H. A. Huan, and T. C. Sum, APL Mater. **2**, 081512 (2014).
[11] J. P. Correa Baena, L. Steier, W. Tress, M. Saliba, S. Neutzner, T. Matsui, F. Giordano, T. J. Jacobsson, A. R. Srimath Kandada, S. M. Zakeeruddin, A. Petrozza, A. Abate, M. K. Nazeeruddin, M. Grätzel, and A. Hagfeldt, Energy Environ. Sci. **8**, 2928 (2015).
[12] N. De Marco, H. Zhou, Q. Chen, P. Sun, Z. Liu, L. Meng, E.-P. Yao, Y. Liu, A. Schiffer, and Y. Yang, Nano Lett. **16**, 1009 (2016).
[13] B. J. Foley, D. L. Marlowe, K. Sun, W. A. Saidi, L. Scudiero, M. C. Gupta, and J. J. Choi, Appl. Phys. Lett. **106**, 243904 (2015).
[14] H.-S. Kim, C.-R. Lee, J.-H. Im, K.-B. Lee, T. Moehl, A. Marchioro, S.-J. Moon, R. Humphry-Baker, J.-H. Yum, J.-E. Moser, M. Grätzel, and N.-G. Park, Sci. Rep. **2**, 591 (2012).
[15] T. G. Kim, S. W. Seo, H. Kwon, J.-H. Hahn, and J. W. Kim, Phys. Chem. Chem. Phys. **17**, 24342 (2015).
[16] C. Li, J. Wei, M. Sato, H. Koike, Z.-Z. Xie, Y.-Q. Li, K. Kanai, S. Kera, N. Ueno, and J.-X. Tang, ACS Appl. Mater. Interfaces **8**, 11526 (2016).
[17] K.-G. Lim, S. Ahn, Y.-H. Kim, Y. Qi, and T.-W. Lee, Energy Environ. Sci. **9**, 932 (2016).
[18] P. Liu, X. Liu, L. Lyu, H. Xie, H. Zhang, D. Niu, H. Huang, C. Bi, Z. Xiao, J. Huang, and Y. Gao, Appl. Phys. Lett. **106**, 193903 (2015).
[19] X. Liu, C. Wang, L. Lyu, C. Wang, Z. Xiao, C. Bi, J. Huang, and Y. Gao, Phys. Chem. Chem. Phys. **17**, 896 (2014).
[20] M. Lo, Z. Guan, T. Ng, C. Chan, and C. Lee, Adv. Funct. Mater. **25**, 1213 (2015).
[21] E. M. Miller, Y. Zhao, C. C. Mercado, S. K. Saha, J. M. Luther, K. Zhu, V. Stevanović, C. L. Perkins, and J. van de Lagemaat, Phys. Chem. Chem. Phys. **16**, 22122 (2014).
[22] P. Schulz, L. L. Whittaker-Brooks, B. A. MacLeod, D. C. Olson, Y.-L. Loo, and A. Kahn, Adv. Mater. Interfaces **2**, 1400532 (2015).
[23] C. Wang, X. Liu, C. Wang, Z. Xiao, C. Bi, Y. Shao, J. Huang, and Y. Gao, J. Vac. Sci. Technol., B: Nanotechnol. Microelectron.: Mater., Process., Meas., Phenom. **33**, 032401 (2015).
[24] Q. Wang, Y. Shao, H. Xie, L. Lyu, X. Liu, Y. Gao, and J. Huang, Appl. Phys. Lett. **105**, 163508 (2014).
[25] H. Xie, X. Liu, L. Lyu, D. Niu, Q. Wang, J. Huang, and Y. Gao, J. Phys. Chem. C **120**, 215 (2016).
[26] X. Zhou, X. Li, Y. Liu, F. Huang, and D. Zhong, Appl. Phys. Lett. **108**, 121601 (2016).
[27] J. Emara, T. Schnier, N. Pourdavoud, T. Riedl, K. Meerholz, and S. Olthof, Adv. Mater. **28**, 553 (2016).
[28] P. Schulz, E. Edri, S. Kirmayer, G. Hodes, D. Cahen, and A. Kahn, Energy Environ. Sci. **7**, 1377 (2014).
[29] E. S. Thibau, A. Llanos, and Z. H. Lu, Appl. Phys. Lett. **108**, 021602 (2016).
[30] F. Hao, C. C. Stoumpos, R. P. H. Chang, and M. G. Kanatzidis, J. Am. Chem. Soc. **136**, 8094 (2014).
[31] See supplementary material at http://dx.doi.org/10.1063/1.4960112 for detailed listings of published ionization energy and work function values as well as a discussion of UPS valence band onset evaluation.
[32] J. Endres, D. A. Egger, M. Kulbak, R. A. Kerner, L. Zhao, S. H. Silver, G. Hodes, B. P. Rand, D. Cahen, L. Kronik, and A. Kahn, J. Phys. Chem. Lett. **7**, 2722 (2016).
[33] S. Meloni, G. Palermo, N. A. Astani, B. F. E. Curchod, M. Graetzel, and U. Roethlisberger, preprint arXiv:1412.3659 (2014).
[34] A. Walsh, J. Phys. Chem. C **119**, 5755 (2015).

[35] C. C. Stoumpos, L. Frazer, D. J. Clark, Y. S. Kim, S. H. Rhim, A. J. Freeman, J. B. Ketterson, J. I. Jang, and M. G. Kanatzidis, J. Am. Chem. Soc. **137**, 6804 (2015).
[36] J. Im, C. C. Stoumpos, H. Jin, A. J. Freeman, and M. G. Kanatzidis, J. Phys. Chem. Lett. **6**, 3503 (2015).
[37] P.-P. Sun, Q.-S. Li, S. Feng, and Z.-S. Li, Phys. Chem. Chem. Phys. **18**, 14408 (2016).
[38] K. T. Butler, J. M. Frost, and A. Walsh, Mater. Horiz. **2**, 228 (2015).
[39] A. Buin, R. Comin, J. Xu, A. H. Ip, and E. H. Sargent, Chem. Mater. **27**, 4405 (2015).
[40] T. M. Koh, K. Fu, Y. Fang, S. Chen, T. C. Sum, N. Mathews, S. G. Mhaisalkar, P. P. Boix, and T. Baikie, J. Phys. Chem. C **118**, 16458 (2014).
[41] F. Hao, C. C. Stoumpos, D. H. Cao, R. P. H. Chang, and M. G. Kanatzidis, Nat. Photonics **8**, 489 (2014).
[42] W. J. Yin, T. Shi, and Y. Yan, Appl. Phys. Lett. **104**, 063903 (2014).
[43] C. C. Stoumpos, C. D. Malliakas, and M. G. Kanatzidis, Inorg. Chem. **52**, 9019 (2013).
[44] A. Pockett, G. E. Eperon, T. Peltola, H. J. Snaith, A. Walker, L. M. Peter, and P. J. Cameron, J. Phys. Chem. C **119**, 3456 (2015).
[45] W. Tress, K. Leo, and M. K. Riede, Adv. Funct. Mater. **21**, 2140 (2011).
[46] Q.-K. Wang, R. Wang, P. Shen, C. Li, Y. Li, L. Liu, S. Duhm, and J. Tang, Adv. Mater. Interfaces **2**, 1400528 (2015).
[47] C. Wang, C. Wang, X. Liu, J. Kauppi, Y. Shao, Z. Xiao, C. Bi, J. Huang, and Y. Gao, Appl. Phys. Lett. **106**, 111603 (2015).